Acetone Chemistry on Oxidized and Reduced TiO_2(110)

Michael A. Henderson*

Interfacial Chemistry and Engineering Group, Pacific Northwest National Laboratory, P.O. Box 999, MS K8-93, Richland, Washington 99352

Received: August 12, 2004; In Final Form: September 21, 2004

The chemistry of acetone on the oxidized and reduced surfaces of TiO_2(110) was examined using temperature-programmed desorption (TPD) and high-resolution electron energy-loss spectroscopy (HREELS). The reduced surface was prepared with about 7% oxygen vacancy sites by annealing in ultrahigh vacuum (UHV) at 850 K, and the oxidized surface was prepared by exposure of the reduced surface to molecular oxygen at 95 K followed by heating the surface to a variety of temperatures between 200 and 500 K. Acetone adsorbs molecularly on the reduced surface with no evidence for either decomposition or preferential binding at vacancy sites. On the basis of HREELS, the majority of acetone molecules adsorbed in an η^1 configuration at Ti^{4+} sites through interaction of lone-pair electrons on the carbonyl oxygen atom. Repulsive acetone−acetone interactions shift the desorption peak from 345 K at low coverage to 175 K as the first layer saturates with a coverage of ~1 ML. In contrast, about 7% of the acetone adlayer decomposes when the surface is pretreated with molecular oxygen. Acetate is among the detected decomposition products but only comprises about one-third of the amount of decomposed acetone, and its yield depends on the temperature at which the O_2-exposed surface was preheated to prior to acetone adsorption. Aside from the small level of irreversible decomposition, about 0.25 ML of acetone is stabilized to 375 K by coadsorbed oxygen. These acetone species exhibit an HREELS spectrum unlike that of η^1-acetone or of any other species proposed to exist from the interaction of acetone with TiO_2 powders. On the basis of the presence of extensive $^{16}O/^{18}O$ exchange between acetone and coadsorbed oxygen in the 375 K acetone TPD state, it is proposed that an acetone−oxygen complex forms on the TiO_2(110) surface through nucleophilic attack of oxygen on the carbonyl carbon atom of acetone. The reaction between acetone and oxygen is initiated at temperatures as low as 135 K based on HREELS. The major decomposition pathway of the acetone−oxygen complex liberates acetone in the 375 K TPD peak. This species may be a key intermediate in acetone thermal and photolytic chemistry on TiO_2 surfaces.

1. Introduction

There is much interest in the thermal[1−10] and photochemical[5,7,9−20] properties of acetone on TiO_2 surfaces. Aside from being a common organic reactant, intermediate, or product in many catalytic processes, acetone is also a common air-borne contaminant. The majority of the studies involving acetone−TiO_2 surface chemistry have involved powder samples, and only Pierce and Barteau examined the interaction of acetone with a TiO_2 single-crystal surface (the (001) termination).[3]

In this study, the chemistry of acetone is probed on the (110) surface of rutile TiO_2 as a function of the redox pretreatment of the surface. This crystal termination is common in rutile powders and represents the thermodynamically most stable face of rutile.[21] When this surface is vacuum annealed, desorption of oxygen initiates reduction of the surface (and bulk), resulting in formation of surface oxygen vacancy sites. Many groups have observed enhanced reactivity of oxygen vacancy sites on TiO_2-(110) compared to the nondefect sites.[21] In contrast to this general impression, results in this study show that acetone does not decompose at vacancy sites on TiO_2(110) nor do these sites enhance the binding of acetone relative to nondefect sites. Instead, acetone reacts with oxygen preadsorbed at vacancy sites. The level of decomposition is equivalent to the prior vacancy coverage and is linked to reactive oxygen species formed on the surface from the interaction of molecular oxygen with vacancies. Aside from inducing decomposition, oxygen also stabilizes acetone on the surface relative to that seen on the reduced surface through two means: by relieving acetone−acetone repulsions and by more strongly coordinating some acetone molecules via formation of an acetone−oxygen complex not observed on the reduced surface. Similarities between the thermal chemistry of acetone and oxygen on TiO_2(110) and photooxidation of acetone on TiO_2 materials suggest that an $O_2^{\delta-}$-related species is the active species that initiates photodecomposition of acetone and not direct hole-mediated processes.

2. Experimental Section

The TiO_2(110) crystal used in this study was obtained from First Reaction with dimensions of 10 × 10 × 1.5 mm. It was epi-polished on both sides to provide maximum thermal contact with the Au-foil-covered heating plate. The surface was cleaned by repeated Ar^+ ion sputtering and annealing (to 850 K) cycles, which also resulted in bulk reduction of the crystal. No contaminants were detected by Auger electron spectroscopy (AES) or secondary-ion mass spectrometry (SIMS) after the sputter/anneal treatments. A sharp (1 × 1) pattern was routinely observed in low-energy electron diffraction (LEED) after annealing. Water temperature-programmed desorption (TPD) was used

* To whom correspondence should be addressed. E-mail: ma.henderson@pnl.gov.

10.1021/jp046357x CCC: $27.50
Published on Web 11/13/2004

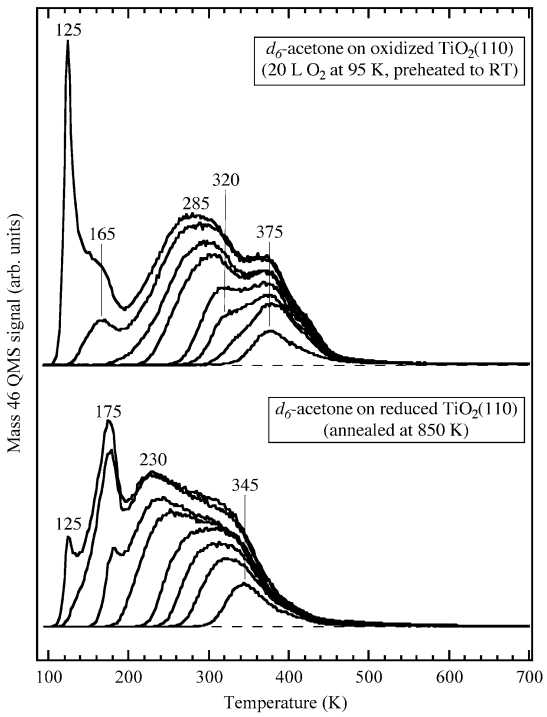

Figure 1. Mass 46 TPD spectra from d_6-acetone adsorbed at 95 K on the reduced (lower set) and oxidized (upper set) surfaces of TiO_2(110). Coverages for both sets of spectra were approximately the same: 0.12, 0.27, 0.38, 0.50, 0.65, 0.77, 0.98, and 1.17 ML.

to detect and quantify surface oxygen vacancies.[22] In this study, the oxygen vacancy population was gauged at about 7%.

Research-grade acetone and d_6-acetone were obtained from Aldrich and further purified using LN2 freeze−pump−thaw cycles. Acetone was exposed to the TiO_2(110) surface using a calibrated directional doser, while oxygen was passed through a LN2 trap and dosed by backfilling the chamber. Acetone TPD experiments were performed with a heating rate of 2 K/s and involved adsorption at 95 K. The reduced surface was prepared by annealing the TiO_2(110) surface in UHV at 850 K before each experiment. In the oxidized surface case, the reduced surface was pretreated with molecular oxygen under various conditions (specified in the text) prior to acetone adsorption. HREELS measurements were performed in the specular scattering geometry using a primary electron beam energy of 9 eV and sample current of <0.1 nA. All HREELS spectra were recorded at 95 K. In this study, '1 ML' is defined based on the areal density five-coordinated Ti^{4+} cation sites on the ideal TiO_2(110) surface (5.2×10^{14} molecules/cm^2).

For dosing, the sample was positioned within 1 mm of the doser tube, and the exposed area was therefore approximately equivalent to the i.d. of the tube. Acetone coverages were estimated from the total exposure of acetone emitted from the calibrated doser during the dose with the assumption that acetone adsorbed on TiO_2(110) at 95 K with near unity sticking probability. This assumption seems reasonable given that the adsorption temperature was about 10 K below the temperature of the onset for multilayer acetone desorption.

3. Results and Discussion

TPD Data. ***Reduced Surface.*** Figure 1 shows two sets of TPD spectra from various coverages of d_6-acetone adsorbed at 95 K on the reduced (lower set) and oxidized (upper set) TiO_2(110) surfaces. The mass 46 QMS cracking fragment (CD_3CO^+) was used because of its prominence in the molecule's mass spectrum. As discussed in the Experimental Section, the reduced surface was obtained after repeated annealing in UHV at 850 K. The level of bulk reduction reached in the crystal in these studies yielded a surface oxygen vacancy population of ~7%. Details on TPD from the oxidized surface are covered in the next section.

TPD of the lowest d_6-acetone coverage on the reduced surface (lower set of Figure 1) yielded a d_6-acetone TPD peak at 345 K. This feature was slightly asymmetric toward higher temperature, with a tail extending out to about 450 K. A simple first-order Redhead analysis[23] for desorption of this coverage of d_6-acetone yields an apparent activation energy of 97 ± 6 kJ/mol using prefactors between 10^{13} and 10^{15} s^{-1}. However, the applicability of the Redhead analysis in this case is questionable because the data suggest coverage dependence in the desorption rate parameters. This coverage dependence is evident by the shift of the desorption profile leading edges toward lower temperature while the trailing edges of the family of traces remained roughly unshifted. The general downward shift in the leading edge of the d_6-acetone TPD spectrum as a function of increasing coverage is a sign of acetone−acetone repulsions that destabilized acetone−Ti^{4+} binding.

The d_6-acetone TPD profile developed a poorly resolved low-temperature component for coverages above about 0.5 ML (the fourth trace in the series of increasing coverages). The desorption peak of this new feature shifted to 230 K with increasing coverage. Broadening of this desorption feature above 0.5 ML suggests that intermolecular repulsions increased relative to those occurring at lower coverage. This change in TPD behavior at 0.5 ML coincides with a situation in which newly adsorbed acetone molecules must occupy adjacent Ti^{4+} sites along the ⟨001⟩ direction. Below 0.5 ML it is possible to minimize acetone−acetone repulsions along the ⟨001⟩ direction with unoccupied sites between nearest-neighbor molecules. The 0.5 ML point might therefore be expected to provide an ordered (2xn) structure in which molecules are coordinated to every other cation site along the rows of cation sites. LEED analysis, however, did not reveal any ordered overlayers of d_6-acetone (other than the (1 × 1); not shown). The absence of higher order LEED patterns from adsorbed acetone might be due to electron-induced effects (decomposition and/or desorption) known to take place for other organics on TiO_2(110).[24−26]

A third d_6-acetone TPD feature appeared at 175 K for coverages above about 0.75 ML on the reduced TiO_2(110) surface (lower portion of Figure 1). This feature saturated at about 1 ML. The TPD peak area of the 175 K state constitutes about 0.2−0.3 ML and therefore is unlikely to have resulted from desorption of a physisorbed layer of d_6-acetone. Using the internal bond angles and distances of acetone and the van der Waals radii of an oxygen atom and a methyl group,[27] the coverage of a physisorbed layer of acetone in which the molecular planes of all the molecules are parallel to the surface is estimated at 7.5×10^{14} molecules/cm^2 (>1.4 ML) based on the TiO_2(110) surface site density. (This coverage would be higher for nonparallel orientations of physisorbed acetone.) Therefore, it seems likely that the 175 K TPD state is not from physisorbed acetone but from molecules registered to the TiO_2(110) surface, either at imperfections in the surface itself or in the acetone adlayer. An example of the former could be the presence of oxygen vacancies, which one might expect to bind an acetone molecule to a greater extent than expected for purely physisorbed acetone. However, the surface density of vacancies (~7%) is too small to account for the amount of d_6-acetone in the 175 K TPD state. Perhaps a more obvious assign-

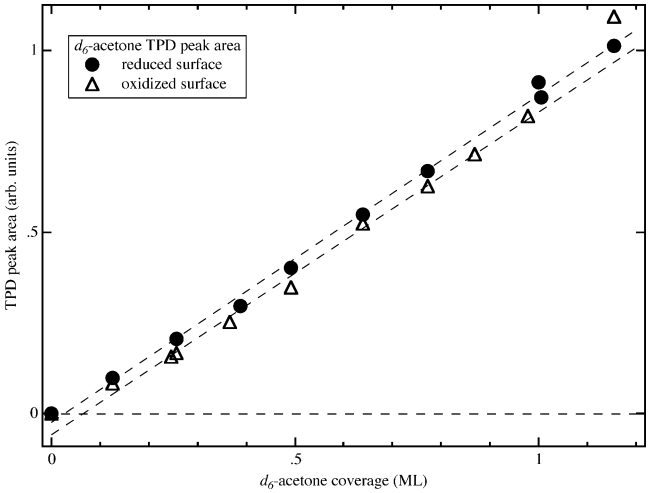

Figure 2. Mass 46 TPD peak areas for various coverages of d_6-acetone adsorbed on the reduced (circles) and oxidized (triangles) surfaces of TiO_2(110). Data obtained from spectra shown in Figure 1.

ment for the 175 K peak is to desorption of that amount of acetone necessary to relieve the intermolecular stresses associated with a highly compressed adlayer in which every available Ti^{4+} site is occupied (i.e., a 1 ML coverage). In this context, the 175 K 'peak' does not signify desorption of acetone from a separate binding site but from a relaxation of the surface after desorption of 20−30% of the saturated first layer. The coincidence of multilayer acetone in TPD at 125 K[28−34] with that of acetone coverages above 1 ML supports this assignment.

No d_6-acetone decomposition products were detected in TPD from the reduced surface. Figure 2 shows the d_6-acetone TPD peak area data for the spectra displayed in the lower portion of Figure 1. Peak area data from the reduced surface (circles) gave a linear fit passing through the origin of the plot. This indicates that within the sensitivity of the TPD measurement all adsorbed d_6-acetone on reduced surface was recovered in TPD as d_6-acetone (i.e., little or no irreversible decomposition of acetone), in agreement with the absence of decomposition products in TPD. There was no evidence in TPD that the 7% oxygen vacancies on the reduced TiO_2(110) surface initiated acetone chemistry under UHV conditions or even bound acetone more strongly than did nondefect sites. Although the TPD spectrum for lowest coverage probed, 0.12 ML, showed a high-temperature tail extending past 400 K, the d_6-acetone TPD spectrum of the same coverage from the oxidized surface (upper portion of Figure 1) also showed the same tail, precluding this feature from arising from interactions with vacancies. The tail more likely arises from d_6-acetone interactions with step sites since these sites may mimic the coordination environment of the acetone−oxygen coadsorbed system (see below). Therefore, it can be concluded that acetone molecules do not interact with oxygen vacancies on the TiO_2(110) with any greater proclivity than they do with nondefect sites. The inability of oxygen vacancies to provide additional stabilization of acetone suggests that the acceptor orbitals of acetone (π^*) are too high in energy to overlap with the electronic states of an oxygen vacancy.

Oxidized Surface. In contrast to results on the reduced surface, exposure of molecular oxygen to reduced TiO_2(110) prior to d_6-acetone adsorption resulted in both stabilization of d_6-acetone on the surface relative to the reduced surface and detectable decomposition. The upper portion of Figure 1 shows the set of d_6-acetone TPD spectra from the oxidized surface with the same coverages used for the reduced surface (lower portion of Figure 1). Spectra from the oxidized surface were not as sensitive to the method of oxidation as to whether the surface was oxidized or reduced, although variations in the decomposition products were detected (discussed below). Several groups have shown that reactive oxygen species are deposited on the TiO_2(110) surface as a result of oxygen exposure to TiO_2(110) surfaces possessing vacancy sites.[35−41] It is particularly important to realize that molecular oxygen does not 'heal' oxygen vacancies in a 1:2 ratio (each oxygen atom in the molecule oxidizing a vacancy) but in a 1:1 ratio, resulting in deposition of an oxygen adatom on the surface.[37,40,41] There is also evidence for molecularly adsorbed O_2 species that are not involved in vacancy oxidation but are stabilized on the surface because of charge transfer from electron density localized at vacancy Ti^{3+} cations.[37−40,42] Because the initial sticking coefficient of O_2 on the reduced surface is ~0.5 at 120 K but substantially decreases for adsorption temperatures above 200 K,[38] it was convenient to saturate the surface with O_2 at 95 K. This required about a 20 L exposure. Prior to adsorption of d_6-acetone at 95 K, the surface was preheated to RT to remove any water adsorbed from background during the O_2 exposure. As will be discussed in elsewhere,[43] coadsorbed water competes aggressively with acetone for adsorption sites on the TiO_2(110) surface. Under these conditions, both molecular and dissociative forms of oxygen exist on the surface.

Using the surface oxidation method described above, the behavior of d_6-acetone in TPD was found to be significantly different on the oxidized surface compared to the reduced surface. The low-coverage feature seen at 345 K on the reduced surface shifted to 375 K for the oxidized surface. This low-coverage TPD feature also filled with more classic first-order desorption behavior (symmetric profile with little coverage dependence in the peak position) than was observed on the reduced surface. A Redhead analysis yields an apparent activation energy of 105 ± 7 kJ/mol for first-order desorption with a prefactor of $10^{14\pm1}$ s^{-1}. This suggests that low-coverage acetone is stabilized on TiO_2(110) by about 8 kJ/mol as a result of the oxygen species deposited on the surface during preoxidation. The 375 K d_6-acetone TPD peak saturated at a coverage of about 0.25 ML.

As will be shown below, the 375 K d_6-acetone TPD feature is the result of a reaction between d_6-acetone and oxygen. It is difficult to draw a correlation between the amount of d_6-acetone in the 375 K TPD peak and the amount of oxygen adsorbed on the surface as a result of O_2 exposure prior to d_6-acetone. It has previously been shown that the saturation uptake of O_2 at 95 K under UHV conditions is about three times the oxygen vacancy coverage.[38] Therefore, the maximum molecular O_2 coverage in these studies would be about 0.21 ML (3 times 0.07 ML). Schaub and co-workers[40] have shown that both molecular and dissociative forms of oxygen exist on TiO_2(110) for low coverages (below the vacancy population) after heating to RT and that these species are highly mobile on TiO_2(110) at RT. At this time, detailed knowledge of the balance between molecular and dissociative oxygen for a saturation O_2 coverage as a function of temperature is not available.

Coverages of d_6-acetone above 0.25 ML on the oxidized TiO_2(110) surface resulted in a second TPD peak that appeared initially at 320 K and shifted to 285 K with increasing coverage (upper portion of Figure 1). Whereas little coverage dependence was detected below a 0.25 ML coverage, evidence for acetone−acetone repulsions appeared in TPD above this coverage on the oxidized surface. The onsets for d_6-acetone desorption were about 35 K higher for the oxidized surface compared to the same coverages on the reduced surface in this coverage range.

These data suggest that intermolecular repulsions are decreased on the oxidized surface, presumably due to the presence of oxygen atoms/molecules occupying Ti^{4+} cation sites and thus decreasing the number of nearest-neighbor acetone−acetone repulsions.

A third d_6-acetone feature appeared in TPD at 165 K from coverages above about 0.75 ML (upper portion of Figure 1). This feature was less intense and broader than the corresponding 175 K feature seen on the reduced surface (lower portion of Figure 1). The fact that the multilayer feature (the 125 K peak) appeared more intense in TPD on the oxidized surface compared to the reduced surface for the same d_6-acetone coverage (1.17 ML) suggests that oxygen atoms/molecules occupy sites that would otherwise have been available to bind d_6-acetone. However, the difference in total amount of d_6-acetone in TPD states above 140 K on the two surfaces was small. Thus, even though the oxidized surface possessed 0.21 ML O_2, the total coverage of d_6-acetone (prior to appearance of the multilayer) was not significantly diminished.

While TPD peak area data from the reduced surface (circles in Figure 2) showed no evidence for unrecovered d_6-acetone, data from the oxidized surface (triangles in Figure 2) did. The data from the oxidized surface also formed a line that paralleled the reduced surface data, but a linear fit of the oxidized surface data intersected the *x*-axis at about 0.065 ML, suggesting this level of irreversible decomposition occurred on the oxidized surface. The coincidence of the *x*-axis intercept with the vacancy coverage prior to oxygen exposure (∼7%) implies that an oxygen species present at this coverage was responsible for the irreversible decomposition. As intriguing as this might seem, it is more likely that only a portion (∼0.07 ML) of the species responsible for the 375 K d_6-acetone TPD feature decomposed irreversibly while most (∼0.25 ML) reversibly librated the parent molecule during heating. This issue will be explored further below.

Figure 3 presents TPD data identifying one of the acetone decomposition products resulting from influence of coadsorbed oxygen. This figure shows mass 42 TPD traces from 0.25 ML d_0-acetone (hereafter referred to simply as acetone) adsorbed on the reduced surface and on the oxygen-exposed surface after various preheating treatments. Mass 42 (CH_2CO^+) was selected because it conveys desorption information from both the parent molecule and a major oxygen-induced decomposition product, acetate. Acetate thermally decomposes on TiO_2(110) to liberate ketene (CH_2CO) between 600 and 700 K (see upper portion of Figure 4). While the mass 14 and 42 QMS signals are the major indicators of ketene, they are comparatively weak for acetone. (The mass 42 signal from acetone is about one-ninth that of the mass 43 signal; see comparison in the bottom portion of Figure 4.) In contrast, the mass 43 signal was strong from acetone and essentially absent from ketene.

While the portions of the mass 42 TPD traces ascribed in Figure 3 to acetone desorption (<500 K) exhibited the same profiles seen from the mass 46 traces for d_6-acetone in Figure 1, additional signal was detected above 500 K for the surfaces pretreated with oxygen. Two 'peaks' were detected in the mass 42 TPD traces at 530 and 660 K, with the latter being the more intense of the two. The feature at 530 K was too weak to identify using correlations with other QMS cracking fragments, but the ratios of mass 14 to mass 42 desorbing at 660 K in the three preoxidation experiments matched that of ketene (see Figure 4). The upper portion of Figure 4 shows the mass 42 TPD trace obtained from a saturation exposure of acetic acid on TiO_2(110) at RT (∼0.5 ML[25,44,45]). The prominent peaks at 600 K resulted from ketene liberation during acetate decomposition, while peaks at 450 and 580 K in the mass 60 spectrum are from acetic acid desorption. Although the peak position for ketene production from a saturated adlayer of acetate was about

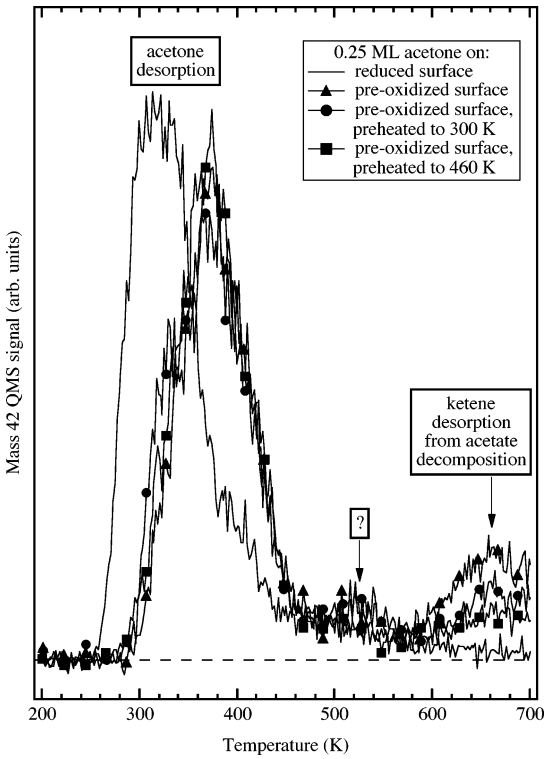

Figure 3. Mass 42 TPD spectra from 0.25 ML acetone adsorbed at 95 K on reduced TiO_2(110) and oxidized TiO_2(110) after various preheating treatments. Features below 500 K are ascribed to acetone desorption, whereas those above 500 K arise from acetone decomposition products.

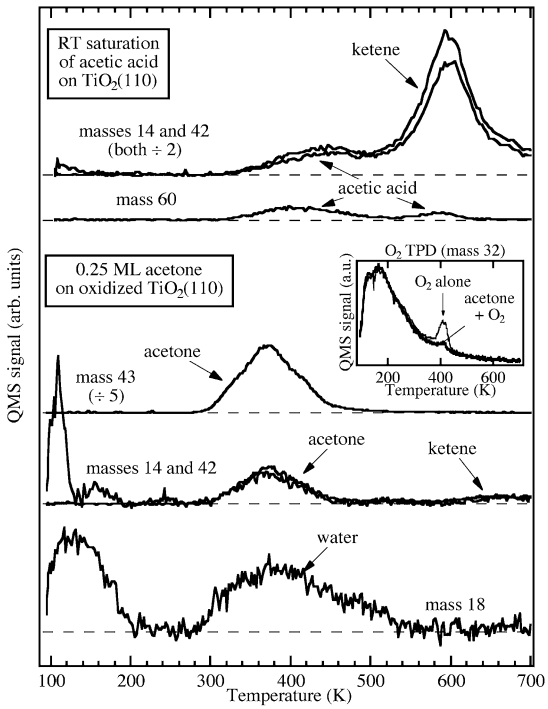

Figure 4. Comparison of TPD traces for various masses resulting from 0.25 ML acetone adsorbed at 95 K on preoxidized TiO_2(110) (lower set) and from a saturation exposure of acetic acid at RT on reduced TiO_2(110) (upper set).

60 K below that observed from the trace amount formed from the reaction of acetone with oxygen, there was still significant desorption signal in the tail of the former peak to suggest that low coverages of acetate on TiO_2(110) decompose above 650 K. The amount of acetate formed from the reaction of acetone and oxygen was about 4% of the total amount of acetate formed from decomposition of a saturated acetate monolayer. Because an appreciable amount of acetate in the latter circumstance recombined with deposited acid protons desorbing as acetic acid, the amount of ketene production from a saturated acetate adlayer on TiO_2(110) was less than 0.5 ML. However, an upper limit on the amount of acetate formed from reaction of acetone with coadsorbed oxygen is 0.02 ML (4% of 0.5 ML), leaving more than 0.04 ML of the decomposed acetone (based on value obtained from Figure 2) unaccounted for. Part of this could come from the unidentified species associated with the 530 K feature.

There was also desorption of about 0.1 ML water above that typically expected from background adsorption during the acetone and oxygen coadsorption experiment shown in bottom portion of Figure 4. The majority of the water desorbed in a broad feature between 300 and 450 K, which is in a thermal region associated with combination of terminal OH groups.[37,46] While the reaction mechanism for acetate formation from acetone and oxygen will be discussed in more detail below, it is clear that if acetate is to form, a C−CH_3 bond in acetone must be broken. The amount of water formed could account for all the H atoms of one methyl group per decomposed acetone molecule, but the carbon is unaccounted for. There was no evidence for carbon left on the surface or for desorption of methane, methanol, formaldehyde, CO, or CO_2. Absence of C_1 species in TPD could be because the amounts formed were below the sensitivity level of these experiments. Coupling products consisting of formation of new C−C bonds from two[1,3,5−7] or more[4] acetone molecules have been observed from acetone chemistry on TiO_2 powders, but no evidence was found in TPD for these reactions on TiO_2(110).

Despite sensitivity limitations that prevented detection of all the decomposition products associated with the reaction of acetone and oxygen, data presented in Figures 2−4 clearly indicate that acetone can be activated on preoxidized TiO_2(110) under UHV conditions. Data in Figure 3 further suggest that the form of oxygen on the surface is important in this chemistry. On TiO_2(110) surfaces possessing oxygen vacancy sites, O_2 adsorbs at 95 K in a precursor state that is perhaps best described as physisorbed.[38] Preheating this O_2 adlayer to temperatures above 200 K results in adsorption into chemisorbed states that are both molecular and dissociative in nature.[38,40] Preheating above 420 K desorbs the molecular form(s), leaving only filled vacancies and a corresponding number of oxygen adatoms.[37,38] Surfaces prepared with each of these O_2-related adlayers showed similar degrees of acetone stabilization, as evidenced by the similar temperature shifts for the 375 K acetone TPD features from the oxidized surfaces. Also, the amounts of acetone recovered in TPD for the three oxidation methods shown were similar to each other. However, there was a detectable change in the amount of acetate formed using the three oxidation conditions of Figure 3. The amount of acetate decreased as the preheating temperature after O_2 exposure was increased, and the signal at 530 K was absent for the surface preheated to 460 K (squares). These data suggest that molecular oxygen may be more important in the conversion of acetone to acetate than is the oxygen adatom formed from O_2 dissociation at vacancies. In agreement with this conclusion, roughly 70% of O_2 that would otherwise desorb from the clean surface at 420 K[38,39]

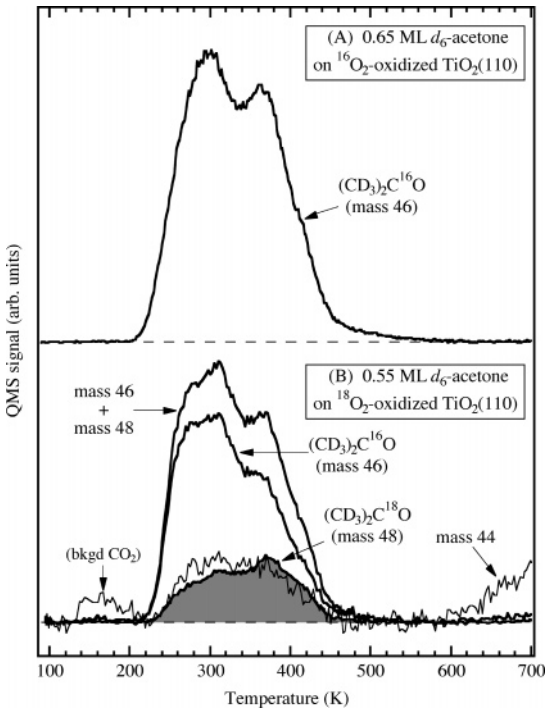

Figure 5. (A) Mass 46 TPD spectrum from coadsorption of 0.65 ML d_6-acetone and 20 L $^{16}O_2$ on TiO_2(110) at 95 K. (B) TPD spectra from mass 44, 46, and 48 and a combination of the latter two for 0.55 ML d_6-acetone coadsorbed with 20 L $^{18}O_2$ on TiO_2(110) at 95 K.

was absent in TPD when O_2 was coadsorbed with acetone (see the inset of Figure 4; the broad feature at ∼180 K was from O_2 adsorbed on the sample holder[46]). Since the level of acetone decomposition was about the same in all three preoxidation experiments, one can therefore speculate that oxygen adatoms are responsible for other acetone decomposition channels because only adatoms are retained on the surface after preheating to above 420 K.[37,38] We have previously shown that physisorbed O_2 reacts with coadsorbed methanol and/or methoxy to form formaldehyde,[26] whereas O adatoms readily dissociate O−H and N−H bonds.[37]

Oxygen Isotope Exchange Studies. A step toward identifying the influence of coadsorbed oxygen on the chemistry of acetone on TiO_2(110) was made using $^{16}O/^{18}O$ isotopic exchange. Figure 5 shows two sets of data. In the upper portion of Figure 5 (labeled A) the mass 46 TPD trace from 0.65 ML d_6-acetone coadsorbed with a 20 L exposure of O_2 (preheated to 200 K) is shown. In the lower portion of Figure 5 (labeled B), the corresponding mass 46 and 48 TPD traces from 0.55 ML d_6-acetone coadsorbed with a 20 L exposure of $^{18}O_2$ (also preheated to 200 K) are shown. (Mass 48 has no significant intensity in the mass spectrum of $(CD_3)_2C^{16}O$.) The presence of a mass 48 TPD signal in both the 305 and 375 K TPD states indicates that a significant amount of oxygen exchange has taken place between $(CD_3)_2C^{16}O$ and coadsorbed $^{18}O_2$, with the 365 K state clearly exhibiting more exchange. Addition of the mass 46 and mass 48 traces (indicated in Figure 5) resulted in the profile expected for TPD of 0.55 ML d_6-acetone on preoxidized TiO_2(110) (compare with the 0.50 ML spectrum in Figure 1). On the basis of the peak areas, about 25% (or 0.14 ML) of the d_6-acetone molecules desorbed with ^{18}O. Again, assuming that the uptake of O_2 was about three times the vacancy population,[38] the total supply of atomic ^{18}O on the surface in this experiment was about 0.42 ML (3 times 2 times 0.07 ML), and about one-third of this ^{18}O reservoir ended up in the desorbing acetone. This high level of exchange indicates that either a stable

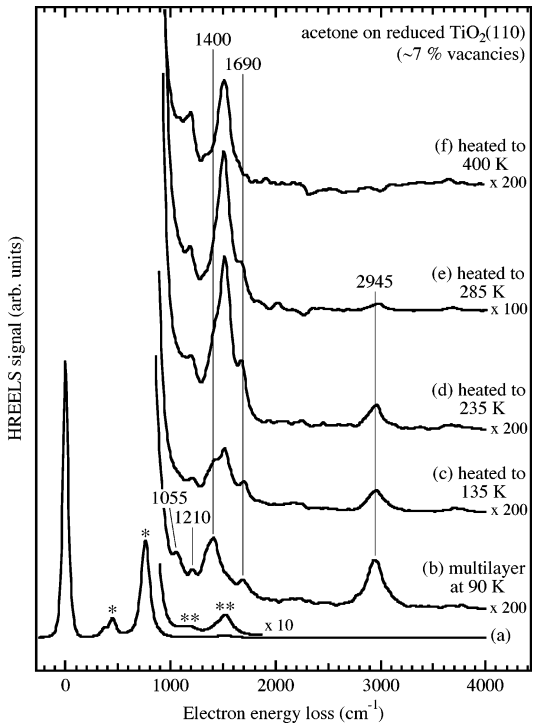

Figure 6. Fourier deconvoluted HREELS spectra for (a) clean TiO_2-(110), (b) a multilayer exposure of acetone on the reduced surface, (c) 'b' heated to 135 K, (d) 'b' heated to 235 K, (e) 'b' heated to 285 K, and (f) 'b' heated to 400 K. Spectra are displaced vertically for clarity.

intermediate or a thermally accessible transition state exists in which the carbonyl carbon atom of acetone interacts with an adsorbed ^{18}O-containing species (e.g., molecular $^{18}O_2$ or an ^{18}O adatom). Because the levels of ^{18}O differ in the two d_6-acetone peaks (at ~305 and 375 K), one can conclude that the species liberating d_6-acetone at 375 K was responsible for the $^{16}O/^{18}O$ exchange but that conversion between the two states was thermally accessible during the course of the TPD experiment. The amount of exchange exceeded one-half of the total d_6-acetone coverage in the 375 K TPD peak.

As an aside, the mass 46 trace in Figure 5 may provide evidence for desorption of a trace amount of ^{18}O-labeled d_2-ketene at >650 K from decomposition of acetates possessing ^{18}O. The mass 44 trace (thin line in the lower portion of Figure 5) also showed a signal in this region but at a level above that expected for d_2-ketene (with ^{16}O) with the balance presumably originating from CO_2 desorption from the sample holder. Alternatively, the mass 46 signal could have resulted from background $C^{16}O^{18}O$ desorption, which could have formed on the chamber walls during $^{18}O_2$ treatment of the surface.

HREELS Data. Insights into the adsorbed state of acetone on reduced TiO_2(110) and from the reaction of acetone and coadsorbed oxygen were obtained using HREELS. The first step in this analysis is the characterization of acetone with the reduced surface.

Reduced Surface. Figure 6 shows HREELS data from a multilayer exposure of acetone on reduced TiO_2(110) followed by analysis after heating to various temperatures. The clean surface spectrum (Figure 6a) shows the prominent phonon losses (labeled with $*$) and the multiple phonon remnant features[47] at 1515 and 1210 cm^{-1} remaining after Fourier deconvolution (labeled with $**$). Wulser and Langell[48] suggested that multiple phonon loss intensity remaining after deconvolution of HREELS spectra from oxides results from two different excitation mechanisms (dipole and impact, for example). Intensity resulting from such multiple excitations should not be removed by Fourier deconvolution since only multiple loss processes resulting from purely dipole scattering will be removed. Absence of the multiple phonon loss after deconvolution of the multilayer spectrum (Figure 6b) illustrates the improbability of exciting and/or detecting an impact scattering event occurring at a buried interface.

Multilayer acetone gave loss peaks at 2945, 1690, 1400, 1350, 1210, and 1055 cm^{-1} that can be assigned to the $\nu_{a/s}(CH_3)$, $\nu(CO)$, $\delta_a(CH_3)$, $\delta_s(CH_3)$, $\nu(CC)$, and $\rho(CH_3)$ modes, respectively. These assignments are consistent with IR measurements of gas-phase acetone and with HREELS measurements of multilayer acetone on other surfaces.[28−30,49] Heating to 135 K desorbed all of the multilayer acetone and a portion of the 175 K state (see Figure 1), leaving nearly a full monolayer on the surface. The most obvious change to the HREELS spectrum after heating to 135 K (Figure 6c) was the appearance of the multiple phonon losses, but additional changes included diminished loss intensities in the $\nu(CC)$ and $\rho(CH_3)$ modes. The loss positions of the remaining features (the $\nu(CH_3)$, $\nu(CO)$, and $\delta(CH_3)$ modes) were not significantly different from those of the multilayer. This is consistent with the predominant form of acetone observed on TiO_2 surfaces at RT being η^1 coordination.[1,2,5,6,8−10] While the $\delta(CH_3)$ modes became too weak to detect after heating to 235 K (Figure 6d), the $\nu(CH_3)$ and $\nu(CO)$ modes were still apparent. These modes shifted in opposite directions (the $\nu(CH_3)$ mode to 2980 cm^{-1} and the $\nu(CO)$ mode to 1660 cm^{-1}) as the acetone monolayer was heated to 285 K. Although these shifts may be ascribed to coverage-dependent changes as the adlayer desorbed, their magnitude was small, indicating that even at low coverage the vibrational modes of acetone were not significantly perturbed by chemisorption of the molecule on the TiO_2(110) surface. Little or no intensity ascribable to acetone remained on the reduced surface after heating to 400 K (Figure 6f), in agreement with the TPD results of Figure 1.

Oxidized Surface. Figure 7 shows HREELS spectra from the interaction of acetone with the oxidized surface of TiO_2(110). Surface oxidation was accomplished by exposing the clean, reduced surface to 40 L O_2 at 95 K followed by preheating to RT prior to adsorption of acetone at 95 K. In a manner similar to that shown in Figure 6, a multilayer exposure on the oxidized surface was preheated to 135, 235, 285, and 400 K. The multilayer spectrum (Figure 7b) was taken from Figure 6b for comparison. The HREELS spectrum after heating a multilayer acetone exposure on the oxidized surface to 135 K (Figure 7c) differed from the same condition on the reduced surface (Figure 6c) in several ways. First, while the relative intensities of the $\nu(CH_3)$ and $\nu(CO)$ modes at 2960 and 1690 cm^{-1} to that of the multiple phonon remnant feature at 1515 cm^{-1} were approximately the same, the 1425 cm^{-1} loss was considerably more intense for the oxidized surface. This relative enhancement was maintained after preheating to 235 K (Figure 7d), at which point there was also a slight relative increase in the intensities of the $\nu(CH_3)$ and $\nu(CO)$ modes. The increases in the relative intensities of these modes compared to those on the reduced surface might be explained simply by the ability of the oxidized surface to stabilize acetone to a greater extent than can the reduced surface. However, the most striking effect is seen after preheating to 285 K (Figure 7e). The 1425 cm^{-1} loss significantly increased in relative intensity, and the 2960 cm^{-1} loss was also considerably more intense than expected based on results from the reduced surface. With the exception of a weak intensity at 1425 cm^{-1}, all losses due to adsorbed acetone were absent after heating the oxidized surface to 400 K (Figure 7f).

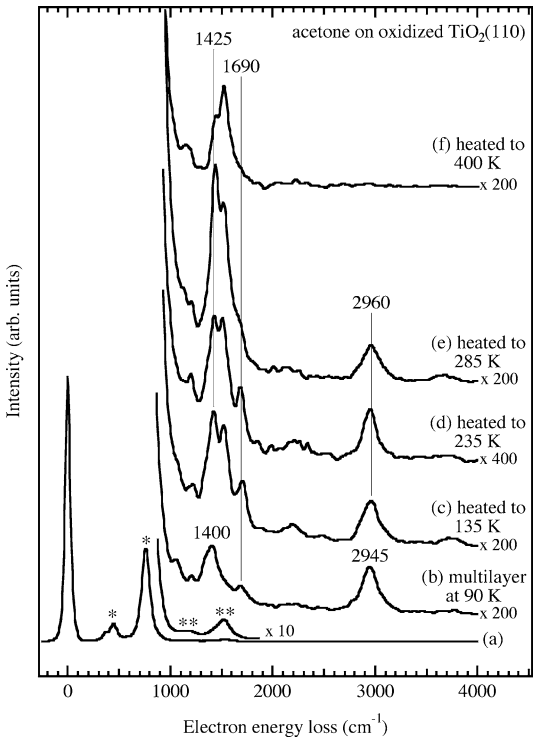

Figure 7. Fourier deconvoluted HREELS spectra for (a) clean TiO_2(110), (b) a multilayer exposure of acetone on the oxidized surface (40 L O_2 at 95 K, preheated to RT), (c) 'b' heated to 135 K, (d) 'b' heated to 235 K, (e) 'b' heated to 285 K, and (f) 'b' heated to 400 K. Spectra are displaced vertically for clarity.

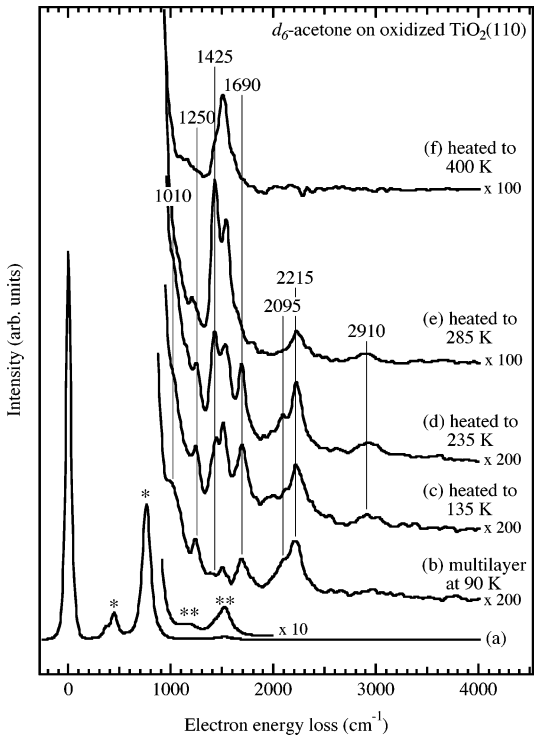

Figure 8. Fourier deconvoluted HREELS spectra for (a) clean TiO_2(110), (b) a multilayer exposure of d_6-acetone on the oxidized surface (40 L O_2 at 95 K, preheated to RT), (c) 'b' heated to 135 K, (d) 'b' heated to 235 K, (e) 'b' heated to 285 K, and (f) 'b' heated to 400 K. Spectra are displaced vertically for clarity.

The intense 1425 cm^{-1} loss in Figure 7e is in the spectral region of several different types of hydrocarbon vibrational modes (e.g., $\delta(CH_3)$, $\nu(C{=}C)$, or $\nu(OCO)$). Assignment of this feature to a $\nu(CH_3)$ mode would seem reasonable based on the similar position of this loss to that of the 1400 cm^{-1} feature of multilayer acetone. However, data in Figure 8 reveals a very different picture. In this figure, a multilayer exposure of d_6-acetone on the oxidized TiO_2(110) surface was heated to the same temperatures as those used in Figures 6 and 7. The losses in the d_6-acetone multilayer spectrum (Figure 8b) at 2215, 2095, 1690, 1250, and 1010 cm^{-1} can be assigned to the $\nu_a(CD_3)$, $\nu_s(CD_3)$, $\nu(CO)$, $\nu(CC)$, and $\delta(CH_3)$ modes, respectively.[28−30,49] The $\rho(CD_3)$ feature was not resolved from the phonon mode at 760 cm^{-1}, which was intense even with a thick molecular multilayer covering the surface. Absence of appreciable signal between 1300 and 1500 cm^{-1} is consistent with the vibrational properties of d_6-acetone. A loss appeared at 1430 cm^{-1} after heating to 135 K (Figure 8c) and grew in relative intensity with additional heating to 285 K (Figure 8d and e). In agreement with the acetone data in Figure 7, this loss diminished to near zero intensity after heating to 400 K (Figure 8f).

The similarity between the 1425 cm^{-1} loss in the d_6-acetone HREELS spectrum for the oxidized surface in Figure 8 and in the acetone HREELS spectrum for the oxidized surface in Figure 7 indicates that this feature is not related to any C−H/C−D vibrations. Aside from CH_3 bending modes, the spectral region between 1300 and 1500 cm^{-1} is typically void of signal for simple organic oxygenates. The 1425 cm^{-1} loss is at least 125 cm^{-1} too low in energy to be associated with typical C═C or C═O bonds and about 200 cm^{-1} too high to be from typical C−C or C−O bonds.[27] A reasonable conclusion is that the species responsible for the 1425 cm^{-1} loss possessed either a perturbed or partially filled C═C or C═O π system such as that seen in adsorbed carboxylic or vinylic species.

Identification of Species Responsible for 375 K TPD State and 1425 cm^{-1} HREELS Feature. HREELS data in Figures 6−8 indicate that acetone and preadsorbed oxygen react to form a unique surface species not observed on the reduced surface. The importance of this interaction is 2-fold. First, it does not result from an interaction of acetone with vacancy sites but from a reaction of acetone with an oxygen species resulting from interaction of O_2 with vacancy sites. The oxygen pretreatment used should oxidize nearly all surface vacancy sites. The most obvious oxygen candidates are either an O adatom or an $O_2^{\delta-}$ species that resulted from charge transfer between a vacancy and O_2, both of which are known to form from the interaction of O_2 with vacancies on TiO_2(110).[37,38,40,42] Second, these results signify the accessibility of complex chemistry occurring during photocatalysis on TiO_2 powders to model studies in UHV on TiO_2(110). As will be discussed in more detail below, photooxidation of acetone on TiO_2 powders likely passes through an acetate intermediate on the way to formate and eventually to CO_2.[10] Results in this study suggest that the initial step in this process is some form of acetone−oxygen complex. Activation of acetone involves reaction of an $O_2^{\delta-}$ species formed after charge transfer from Ti^{3+} to O_2.

The intense 1425 cm^{-1} loss in Figures 7 and 8 reflects the key intermediate in the reaction of acetone and oxygen on TiO_2-(110). While its thermal behavior is closely linked to that of the 375 K acetone TPD peak (Figure 1), its spectral position is unlike anything in the acetone vibrational spectrum. As discussed above, this loss is insensitive to the H/D isotopic character of acetone and therefore must arise from vibrations associated with C and O. Figure 9 shows potential candidate species that might arise from the reaction of acetone and coadsorbed oxygen to give an intense loss feature at 1425 cm^{-1}.

The major form of acetone on TiO_2 surface is coordinated to Ti^{4+} sites through the oxygen lone-pair electrons in an η^1

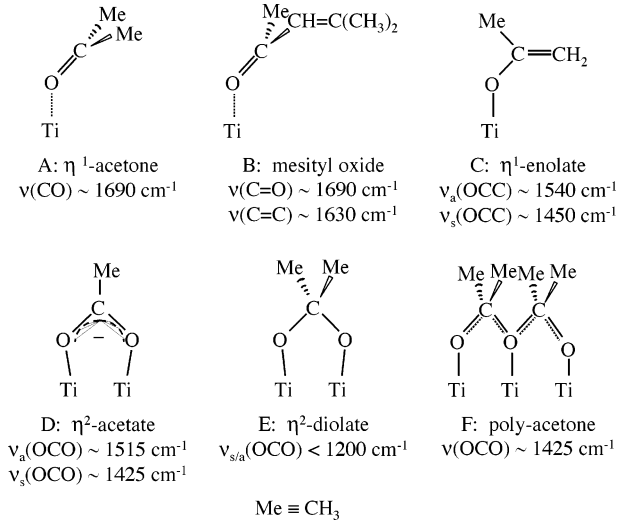

Figure 9. Candidate species resulting from the interaction of acetone with TiO_2(110).

configuration (Figure 9A). The energy of the ν(CO) mode of η^1 acetone is red shifted only slightly from the gas-phase value. IR studies on pure rutile[1] and on mostly anatase (e.g., Degussa P25)[2,5,6,8−10] TiO_2 powders show that η^1-acetone is prevalent after acetone exposure at RT but desorbs or reacts on heating. This form of adsorbed acetone was observed exclusively on the reduced TiO_2(110) surface (Figure 6) and dominated on the oxidized surface at low temperature and high coverage (Figures 7c and 8c). This species is weakly bound and desorbs from TiO_2(110) below 350 K based on correlation of TPD data in Figure 1 with HREELS data in Figure 6.

Powder TiO_2 studies indicate that acetone can be activated to form coupled products. One such product, mesityl oxide ($(CH_3)_2C{=}C{-}C(=O){-}CH_3$), shown in Figure 9B, results from dehydrative coupling of two acetones[1,5,6,9] based on IR modes in the 1600−1700 cm^{-1} region associated with ν(C═C) and ν(C═O) modes. (The hydrated analogue of this ($(CH_3)_2C(-OH){-}CH_2{-}C(=O){-}CH_3$) has also been proposed.[6]) Evidence for acetone coupling products on other TiO_2 surface have also been seen in TPD.[3,4] In the case of TiO_2(110), there was no evidence in TPD or HREELS for acetone coupling. It is unlikely that formation of mesityl oxide (or any other form of coupled acetone product involving new C−C bonds) should be reversible toward acetone to the extent depicted by the 375 K TPD state. Although formation of a small amount (~0.04 ML) could account for the missing products of the reaction of acetone and oxygen, it is clear that such species are not responsible for the 1425 cm^{-1} loss and the 375 K acetone TPD feature. The ν(C═C) mode of a high-coverage acetone coupling product might be masked by the phonon remnant mode at 1515 cm^{-1} (labeled with ∗∗ in the HREELS figures), but there was no evidence for vinylic ν(C−H) losses which generally are observed above 3000 cm^{-1}.

Acetone enolate (Figure 9C) is also another possibility for the 1425 cm^{-1} feature. This species forms from either acid- or base-catalyzed abstraction of a hydrogen from one of the acetone methyl groups and has been proposed as an intermediate in acetone chemistry on a variety of oxide materials.[50−60] In IR studies of acetone on TiO_2, Martin et al.[2] and Griffiths and Rochester[1] assigned features at 1540 and 1450 cm^{-1} to the ν_a(OCC) and ν_s(OCC) modes, respectively, of this species. Only Griffiths and Rochester[1] used d_6-acetone, and these authors found that the 1540 and 1450 cm^{-1} features were not shifted. Both groups commented on the similarity of these energies with those of the ν_s(OCO) and ν_a(OCO) modes of η^2-carboxylates (such as acetate illustrated in Figure 9D). A similar conclusion was reached by Hanson et al.[54] for the 1562 and 1445 cm^{-1} bands observed from acetone on γ-Al_2O_3 powder. These authors concluded that these features were not due to acetone enolate because the ν_s(OCC) and ν_a(OCC) modes of enolate salts did not match these features. Instead, Hanson et al. also suspected these features were due to carboxylates. For acetone and d_6-acetone studies on α-Fe_2O_3,[61] MgO,[50,51] NiO,[50,51] and SnO_2,[52] features at 1550 and 1450 cm^{-1} were assigned to a carboxylate (acetate) with the aid of comparisons from acetic acid adsorption. Acetate was also found as a surface product from the decomposition of acetone on the oxygen precovered surfaces of Rh(111)[62] and Ir(111)[63] as well as on clean Ni(111).[64] In these studies, acetate was discerned based on comparison with the same product from acetic acid adsorption.

Acetone enolate (Figure 9C) has been observed on Ni(111)[64] and also on oxygen precovered Ag(111)[65] and Ag(110).[49] In each case, the distinguishing features of this species were a ν(C−O) mode at ~1300 cm^{-1} and a ν(C═C) mode at ~1550 cm^{-1}. (The latter was not detected in the O/Ag(111) case.) Most notable in these studies was the absence of any signal in the 1400−1500 cm^{-1} region for the deuterated analogues. An acetone enolate species also possesses an ν(C−H) mode above 3000 cm^{-1} due to the ═CH_2 group, as seen in the HREELS example on Ag(110)[49] or in IR analysis of alkali enolate salts.[66] No intensity was observed in this region on TiO_2(110) (see Figures 7 and 8). On the basis of these observations and on the IR spectral characteristics of acetone enolate complexes (see references in Sim et al.[64]) and salts,[66,67] the conclusion can be made that the acetone-related species responsible for the 1425 cm^{-1} loss on TiO_2(110) is not an acetone η^1(O)-enolate (Figure 9C). Similarly, acetone η^1(C)-enolate[68] and bridging η^2(C,O)-enolate[69,70] can be excluded as candidates based on comparisons with the vibrational spectra of organometallic complexes possessing these ligands. Aside from the lack of consistency in the vibrational spectra, it is difficult to mechanistically conceive how an acetone enolate species, formed by H abstraction from acetone methyl group by a surface oxygen species, should regenerate acetone, especially since combination of terminal OH groups is facile at temperatures below 350 K on TiO_2(110).[37,46] (It is clear that bridging oxygen atoms do not abstract H atoms from acetone methyl groups because these sites appear to play no role in acetone chemistry on the reduced surface.) H/D exchange (to be discussed below) does appear to take place on the oxidized surface. However, separate TPD studies[43] involving coadsorbed water show that the extent of H/D exchange is small even under conditions when excess water is present. This suggests that H/D exchange is not a result of recombination of high coverages of stable enolate and OH but more likely the result of a channel involving a transition state thermally accessible during acetone desorption.

Results from the interaction of acetone with oxygen-covered Ag(110)[49] and Ag(111)[65] also support the formation of an η^2-diolate shown in Figure 9E. Decomposition of this species to liberate acetone involved oxygen-atom scrambling with the preadsorbed O on Ag(110),[49] which would explain the TPD results of Figure 5. However, this species can be excluded because its ν_a(OCO) and ν_s(OCO) modes are both below 1200 cm^{-1} and no signal is expected from the deuterated analogue between 1500 and 1400 cm^{-1}.

Acetate (Figure 9D) can also be ruled out as the species responsible for the 1425 cm^{-1} feature in Figures 7 and 8.

Although HREELS data for acetate on TiO_2(110) is not available, Rotzinger et al.[71] recently studied acetate adsorbed on TiO_2(110) using FTIR. The characteristic ν_a(OCO), ν_s(OCO), and $\delta(CH_3)$ modes were observed at 1548/1512, 1422, and 1350 cm^{-1}, respectively. Only the latter two modes should be detected for acetate in its preferred C_{2v} adsorption symmetry on TiO_2(110)[21,25] based on HREELS selection rules.[72] The similarity of the ν_s(OCO) mode of acetate with the 1425 cm^{-1} loss in Figures 7 and 8 is suggestive of acetate formation from the interaction of acetone with oxygen on TiO_2(110). Such an assignment would concur with the acetone−powder oxide studies mentioned above. However, the amount of acetate formed from the interaction of acetone and oxygen was small (~0.02 ML) based on TPD (Figure 4), and the thermal behavior of the 1425 cm^{-1} loss tracked the acetone desorption at 375 K peak and not the thermal behavior of acetate that decomposed above 550 K (Figure 4). Mechanistically, it seems improbable that the 375 K acetone feature could result from a reaction-limited process involving acetate given the much greater stability of acetate on TiO_2(110) relative to acetone. Kim and Barteau[73] observed formation of acetone from a bimolecular reaction of acetates on the {114}-faceted surface of TiO_2(001), but this reaction only takes place above 650 K and only for this faceted surface in which highly uncoordinated Ti^{4+} cations are present. Observations of the formation of acetate from decomposition of acetone on TiO_2 powders based on IR data may have missed the existence of a surface species with vibrational properties that resemble acetate but in fact is an intermediate between acetone and acetate. In the case of TiO_2(110), the arrangement of surface sites may favor formation of this intermediate but at the same time limits the forward reaction to acetate, while the opposite may be the case on TiO_2 powders.

While no acceptable candidates for the species responsible for the 1425 cm^{-1} feature, which is linked to the 375 K acetone TPD state, present themselves from the literature, the characteristics of this species are sufficiently distinct to offer the following as a possibility. Decomposition of this species must preferentially liberate molecular acetone upon decomposition, facilitate extensive oxygen exchange with coadsorbed $^{18}O_2$, and possess a structure that affords a vibrational mode at 1425 cm^{-1} that is not C−H related. Figure 8F presents 'poly-acetone' as a possible species that meets these requirements. In this model, an oxygen atom (or molecule) from coadsorbed oxygen attacks the carbonyl carbon atom of a neighboring η^1-acetone molecule, causing rehybridization of the carbonyl's π-system. The resulting structure must be unlike that of the diolate species shown in Figure 9E, which possesses C−O single bonds. C−O single bonds should not yield a stretching mode as high as 1425 cm^{-1}. One way to rationalize C−O bonds that appear half-order between single and double would be if a π-system were formed. Such a system may account for an intense ν(CO) between that of a single bond (~1000 cm^{-1}) and a double bond (~1700 cm^{-1}). The structure of the TiO_2(110) surface along the ⟨001⟩ direction (along the rows of cation sites) may enable continuance of this rehybridization to the next η^1-acetone molecule and so on. HREELS results in Figures 7 and 8 indicate that the 1425 cm^{-1} loss grew in intensity at the expense of the 1690 cm^{-1} loss of η^1-acetone as the temperature was raised above 135 K.

Assuming linear chains of acetone, such as that shown in Figure 9F, are responsible for the unusual behavior of the acetone + oxygen coadsorbed system, then the high degree of $^{16}O/^{18}O$ exchange between acetone and oxygen suggests that the chains are relatively short such that the end groups, where initiation occurs, are of comparable contribution to the chains compared to the rest. Decomposition of the chain would preferentially yield acetone but with either end of the chain leaving an oxygen atom on the surface. Additionally, decomposition of the end of the chain provides a natural transition for formation of acetate (Figure 9D) via demethylation. Additional studies using techniques not available to this study (e.g., scanning probe analysis) are required in order to confirm or reject this model.

Relevance to Heterogeneous Photooxidation of Acetone. There is a similarity between one of the thermal reaction products observed from the coadsorption of acetone and oxygen on TiO_2(110) and a photochemical reaction intermediate detected by Coronado et al.[10] during acetone photooxidation on TiO_2 powder. In both cases, acetate species are observed. This similarity suggests that a viable reaction pathway in both the thermal and photochemical reactions on TiO_2 may involve nucleophilic attack of an $O_2^{\delta-}$ species on an acetone molecule. Results from Figure 3 suggest that the yield of acetate from the reaction of acetone and oxygen was sensitive to the conditions in which the surface was exposed to oxygen, while the overall extent of acetone decomposition was not. A better understanding of the selectivity between acetate and other products awaits identification of the other reaction products. Nevertheless, it appears that a surface rich in molecularly adsorbed O_2 preferentially yields acetate. If this similarity between the thermal reaction on TiO_2(110) and the photochemical reaction on other TiO_2 surfaces holds true, this would be an example of the electron channel of photoexcited TiO_2 taking an active role in photooxidation of organics along with the hole channel.

H/D Exchange. An interesting occurrence in the HREELS data of d_6-acetone (Figure 8) not discussed above is the presence of a 2910 cm^{-1} loss after desorption of the d_6-acetone multilayer by heating to 135 K. This loss is in the region traditionally attributed to C−H stretches, although one might assign the feature to a combination mode involving the 715 cm^{-1} phonon loss of TiO_2(110) and the $\nu(CD_3)$ modes of adsorbed d_6-acetone. The former is the better explanation since no such combination mode was detected in the multilayer spectrum (Figure 8b), which still possessed significant intensity in the 715 cm^{-1} feature. Independent TPD studies involving coadsorption of d_6-acetone and H_2O (as well as acetone and D_2O) on TiO_2(110) show that exchange does take place. While these data are reserved for a future publication,[43] the data in Figure 8 supports the existence of an acetone enolate intermediate on TiO_2(110). Acetone enolate has been shown to be responsible for H/D exchange on many surfaces.[1,51,52,54,60,61,74] The source of H in these studies was ascribed to OH groups and in the present study was likely from background water. It is interesting that the ν(CH) mode at 2910 cm^{-1} was present even at 135 K, but its relative intensity did not increase with additional heating. Perhaps these observations indicate that the acetone enolate only forms at minority sites such as step edges.

4. Conclusions

Acetone does not decompose under UHV conditions on a TiO_2(110) surface possessing 7% oxygen vacancy sites. On the basis of HREELS, the major adsorption state on this surface is an η^1-acetone species presumably bound at Ti^{4+} sites via the lone pair on the oxygen atom of acetone. TPD indicates strong coverage dependence in the binding energy of acetone, especially near saturation of the first layer at one acetone per surface Ti^{4+} site. No TPD state associated with vacancies was observed. In contrast, preoxidation of the surface with O_2 led to about 7% acetone decomposition along with significant changes in

the TPD and HREELS. Coadsorbed oxygen stabilized 0.25 ML of acetone to about 40 K higher desorption temperature than that observed on the surface possessing vacancies. Preoxidation with $^{18}O_2$ showed extensive oxygen exchange into this stabilized acetone state. The HREELS spectrum of this acetone state was unlike that of η^1-acetone or any other form of adsorbed acetone proposed in the literature and is tentatively assigned to polymerized acetone initiated by coadsorbed oxygen. Decomposition of this species preferentially liberates acetone in TPD but is also responsible for the 7% irreversible decomposition referred to above. About one-third of the observed decomposition (0.02 ML) resulted in acetate, but the remainder was unassigned. Acetate was favored when preoxidation was done at 95 K but diminished as the oxygen-exposed surface was preheated to RT and above. Similarities with results on the photooxidation of acetone on TiO_2 powders suggest that both oxidation and photooxidation of acetone to acetate is initiated by $O_2^{\delta-}$, which is formed in this study from O_2 exposure at low temperature on TiO_2(110).

Acknowledgment. This work was funded by the Office of Basic Energy Sciences, Division of Materials Sciences and Chemical Sciences. Pacific Northwest National Laboratory is a multiprogram national laboratory operated for the U.S. Department of Energy by the Battelle Memorial Institute under contract DE-AC06-76RLO 1830. The research reported here was performed in the William R. Wiley Environmental Molecular Science Laboratory, a Department of Energy user facility funded by the Office of Biological and Environmental Research.

References and Notes

(1) Griffiths, D. M.; Rochester, C. H. *J. Chem. Soc., Faraday Trans. 1* **1978**, *74*, 403.
(2) Martin, C.; Martin, I.; Rives, V. *J. Catal.* **1994**, *145*, 239.
(3) Pierce, K. G.; Barteau, M. A. *J. Org. Chem.* **1995**, *60*, 2405.
(4) Luo, S.; Falconer, J. L. *J. Catal.* **1999**, *185*, 393.
(5) El-Maazawi, M.; Finken, A. N.; Nair, A. B.; Grassian, V. H. *J. Catal.* **2000**, *191*, 138.
(6) Zaki, M. I.; Hasan, M. A.; Pasupulety, L. *Langmuir* **2001**, *17*, 768.
(7) Xu, W.; Raftery, D. *J. Catal.* **2001**, *204*, 110.
(8) Hasan, M. A.; Zaki, M. I.; Pasupulety, L. *J. Phys. Chem. B* **2002**, *106*, 12747.
(9) Xu, W.; Raftery, D.; Francisco, J. S. *J. Phys. Chem. B* **2003**, *107*, 4537.
(10) Coronado, J. M.; Kataoka, S.; Tejedor-Tejedor, I.; Anderson, M. A. *J. Catal.* **2003**, *219*, 219.
(11) Pearl, J.; Ollis, D. F. *J. Catal.* **1992**, *136*, 554.
(12) Sauer, M. L.; Ollis, D. F. *J. Catal.* **1994**, *149*, 81.
(13) Yu, J. C.; Lin, J.; Lo, D.; Lam, S. K. *Langmuir* **2000**, *16*, 7304.
(14) Vorontsov, A. V.; Stoyanova, I. V.; Kozlov, D. V.; Simagina, V. I.; Savinov, E. N. *J. Catal.* **2000**, *189*, 360.
(15) Choi, W.; Ko, J. Y.; Park, H.; Chung, J. S. *Appl. Catal. B* **2001**, *31*, 209.
(16) Attwood, A. L.; Edwards, J. L.; Rowlands, C. C.; Murphy, D. M. *J. Phys. Chem. A* **2003**, *107*, 1779.
(17) Chang, C.-P.; Chen, J.-N.; Lu, M.-C. *J. Environ. Sci. Health, Part A* **2003**, *A38*, 1131.
(18) Coronado, J. M.; Zorn, M. E.; Tejedor-Tejedor, I.; Anderson, M. A. *Appl. Catal. B* **2003**, *43*, 329.
(19) Kozlov, D.; Bavykin, D.; Savinov, E. *Catal. Lett.* **2003**, *86*, 169.
(20) Raillard, C.; Hequet, V.; Le Cloirec, P.; Legrand, J. *J. Photochem. Photobiol., A* **2004**, *163*, 425.
(21) Diebold, U. *Surf. Sci. Rep.* **2003**, *48*, 53.
(22) Henderson, M. A. *Surf. Sci. Rep.* **2002**, *46*, 1.
(23) Redhead, P. A. *Vacuum* **1962**, *12*, 203.
(24) Chambers, S. A.; Thevuthasan, S.; Kim, Y. J.; Herman, G. S.; Wang, Z.; Tober, E.; Ynzunza, R.; Morais, J.; Peden, C. H. F.; Ferris, K.; Fadley, C. S. *Chem. Phys. Lett.* **1997**, *267*, 51.
(25) Guo, Q.; Cocks, I.; Williams, E. M. *J. Chem. Phys.* **1997**, *106*, 2924.
(26) Henderson, M. A.; Otero-Tapia, S.; Castro, M. E. *Faraday Discuss.* **1999**, *114*, 313.
(27) *Handbook of Chemistry and Physics*, 57th ed.; Weast, R. C., Ed.; CRC Press: Cleveland, OH, 1977.
(28) Avery, N. R. *Surf. Sci.* **1983**, *125*, 771.
(29) Anton, A. B.; Avery, N. R.; Toby, B. H.; Weinberg, W. H. *J. Am. Chem. Soc.* **1986**, *108*, 684.
(30) Vannice, M. A.; Erley, W.; Ibach, H. *Surf. Sci.* **1991**, *254*, 1.
(31) Kusunoki, I.; Sakashita, M.; Takaoka, T.; Range, H. *Surf. Sci.* **1996**, *357−358*, 693.
(32) Sparks, S. C.; Szabo, A.; Szulczewski, G. J.; Junker, K.; White, J. M. *J. Phys. Chem. B* **1997**, *101*, 8315.
(33) Dinger, A.; Lutterloh, C.; Biener, J.; Küppers, J. *Surf. Sci.* **1999**, *437*, 116.
(34) Syomin, D.; Koel, B. E. *Surf. Sci.* **2002**, *498*, 53.
(35) Lu, G.; Linsebigler, A.; Yates, J. T., Jr. *J. Chem. Phys.* **1995**, *102*, 4657.
(36) Rusu, C. N.; Yates, J. T., Jr. *Langmuir* **1997**, *13*, 4311.
(37) Epling, W. S.; Peden, C. H. F.; Henderson, M. A.; Diebold, U. *Surf. Sci.* **1998**, *412/413*, 333.
(38) Henderson, M. A.; Epling, W. S.; Perkins, C. L.; Peden, C. H. F.; Diebold, U. *J. Phys. Chem. B* **1999**, *103*, 5328.
(39) Perkins, C. L.; Henderson, M. A. *J. Phys. Chem. B* **2001**, *105*, 3856.
(40) Schaub, R.; Wahlstroem, E.; Ronnau, A.; Laegsgaard, E.; Stensgaard, I.; Besenbacher, F. *Science* **2003**, *299*, 377.
(41) Henderson, M. A.; White, J. M.; Uetsuka, H.; Onishi, H. *J. Am. Chem. Soc.* **2003**, *125*, 14974.
(42) Wahlstroem, E.; Vestergaard, E. K.; Schaub, R.; Ronnau, A.; Vestergaard, M.; Laegsgaard, E.; Stensgaard, I.; Besenbacher, F. *Science* **2004**, *303*, 511.
(43) Henderson, M. A. *Langmuir*, submitted for publication.
(44) Fukui, K.-I.; Iwasawa, Y. *Surf. Sci.* **2000**, *464*, L719.
(45) Idriss, H.; Legare, P.; Maire, G. *Surf. Sci.* **2002**, *515*, 413.
(46) Henderson, M. A.; Epling, W. S.; Peden, C. H. F.; Perkins, C. L. *J. Phys. Chem. B* **2003**, *107*, 534.
(47) Henderson, M. A. *Surf. Sci.* **1996**, *355*, 151.
(48) Wulser, K. W.; Langell, M. A. *Phys. Rev. B* **1993**, *48*, 9006.
(49) Ayre, C. R.; Madix, R. J. *J. Am. Chem. Soc.* **1995**, *117*, 2301.
(50) Miyata, H.; Wakamiya, M.; Kubokawa, Y. *J. Catal.* **1974**, *34*, 117.
(51) Miyata, H.; Toda, Y.; Kabokawa, Y. *J. Catal.* **1974**, *32*, 155.
(52) Thornton, E. W.; Harrison, P. G. *J. Chem. Soc., Faraday Trans. 1* **1975**, *71*, 2468.
(53) Ziolkowski, J.; Wiltowski, T. *J. Catal.* **1984**, *90*, 329.
(54) Hanson, B. E.; Wieserman, L. F.; Wagner, G. W.; Kaufman, R. A. *Langmuir* **1987**, *3*, 549.
(55) Vohs, J. M.; Barteau, M. A. *J. Phys. Chem.* **1991**, *95*, 297.
(56) Iglesia, E.; Barton, D. G.; Biscardi, J. A.; Gines, M. J. L.; Soled, S. L. *Catal. Today* **1997**, *38*, 339.
(57) Sanz, J. F.; Ovideo, J.; Marquez, A.; Odriozola, J. A.; Montes, M. *Angew. Chem., Int. Ed.* **1999**, *38*, 506.
(58) Zaki, M. I.; Hasan, M. A.; Al-Sagheer, F. A.; Pasupulety, L. *Langmuir* **2000**, *16*, 430.
(59) Gutierrez-Sosa, A.; Evans, T. M.; Parker, S. C.; Campbell, C. T.; Thornton, G. *Surf. Sci.* **2002**, *497*, 239.
(60) Xu, M.; Wang, W.; Hunger, M. *Chem. Commun.* **2003**, 722.
(61) Busca, G.; Lorenzelli, V. *J. Chem. Soc., Faraday Trans. 1* **1982**, *78*, 2911.
(62) Houtman, C.; Barteau, M. A. *J. Phys. Chem.* **1991**, *95*, 3755.
(63) Karseboom, S. G.; Davis, J. E.; Mullins, C. B. *Surf. Sci.* **1997**, *383*, 173.
(64) Sim, W.-S.; Li, T.-C.; Yang, P.-X.; Yeo, B.-S. *J. Am. Chem. Soc.* **2002**, *124*, 4970.
(65) Sim, W. S.; King, D. A. *J. Phys. Chem.* **1996**, *100*, 14794.
(66) Lochmann, L.; Rajib, L. D.; Trekoval, J. *J. Organomet. Chem.* **1978**, *156*, 307.
(67) Nonella, M.; Suter, H. U. *J. Phys. Chem. A* **1999**, *103*, 7867.
(68) Suzaki, Y.; Yagyu, T.; Yamamura, Y.; Mori, A.; Osakada, K. *Organomet.* **2002**, *21*, 5254.
(69) Gallo, E.; Ragaini, F.; Cenini, S.; Demartin, F. *J. Organomet. Chem.* **1999**, *586*, 190.
(70) Ruiz, J.; Rodríguez, V.; Cutillas, N.; Pardo, M.; Pérez, J.; López, G. *Organometallics* **2001**, *20*, 1973.
(71) Rotzinger, F. P.; Kesselman-Truttmann, J. M.; Hug, S. J.; Shklover, V.; Grätzel, M. *J. Phys. Chem. B* **2004**, *108*, 5004.
(72) Ibach, H.; Mills, D. L. *Electron Energy Loss Spectroscopy and Surface Vibrations*; Academic Press: New York, 1982.
(73) Kim, K. S.; Barteau, M. A. *J. Catal.* **1990**, *125*, 353.
(74) Young, R. P.; Sheppard, N. *J. Catal.* **1971**, *20*, 333.